PRECODING AND POSTCODING SCHEMES FOR WIRELESS VIDEO TRANSMISSION IN OVERLOADED MIMO SYSTEMS

Koji Tashiro, Leonardo Lanante, Masayuki Kurosaki, and Hiroshi Ochi

Graduate School of Computer Science and Systems Engineering, Kyushu Institute of Technology, Japan

ABSTRACT

Image and video transmission is highly expected to proliferate with the wide spread of Wi-Fi devices and the introduction of multiple-input multiple-output (MIMO) systems. This paper proposes a novel precoder for video transmission in overloaded MIMO systems, which is based on an eigenbeam space division multiplexing (E-SDM) technique. This paper also proposes a low complexity postcoder, which detects some of data symbols by a linear approach and the others by a prevoting vector cancellation (PVC) approach. It is shown from simulation results that the proposed precoder and postcoder achieve 40 dB in peak signal-to-noise ratio while reducing the computational complexity by over 61% compared to the conventional PVC-based detection when received signal-to-noise ratio is higher than 10 dB.

***Index Terms*—** Overloaded MIMO, Video Transmission, E-SDM, Joint Source-Channel Coding

1. INTRODUCTION

Image and video transmission has become one of the major applications of wireless communication systems due to the wide spread of Wi-Fi devices and the development of multiple-input multiple-output (MIMO) technology. MIMO systems raise the channel capacity through multiple antennas, making it possible to satisfy the requirement of high data rate for image and video transmission [1]. The number of antennas deployed in access points (base stations) can be increased without space restrictions [2]. In contrast, the number of antennas implemented in mobile terminals is strictly limited by the space for antenna elements [3]. Hence, overloaded MIMO systems have been considered, where the number of spatial streams (data symbols) to be transmitted is larger than that of receive antennas [4]. Linear detection schemes such as zero-forcing (ZF) and minimum mean square error (MMSE) do not work for overloaded MIMO channels since the system has fewer equations than unknowns. It is true that maximum likelihood detection (MLD) is an optimal method and shows the best performance even in overloaded MIMO systems, but its computational complexity is extremely high. It is practically infeasible for most of mobile devices to employ MLD from the perspectives of hardware implementation and power consumption. Low complexity detectors for overloaded MIMO systems have been proposed. A prevoting vector cancellation (PVC) approach was presented in [5, 6], which reduced the the number of candidate symbol vectors for MLD taking advantage of a linear detector. An efficient generalized sphere decoder with column reordering was proposed in [7].

An essential characteristic of the current image and video coding standards is unequal significance in a code stream. A scalable code stream consists of multiple layers whose contribution to image quality is unequal. The design of efficient coding schemes that simultaneously take into account both source characteristics and transmission techniques is well known as joint source-channel coding, which is capable of enhancing image quality even in the presence of errors inside the code stream. An unequal power allocation (UPA) scheme for the transmission of joint photographic experts group (JPEG) compressed images over MIMO systems was presented in [8]. The concept of UPA is to assign more power to visually important information bits to protect them from errors. A precoding scheme for video transmission was developed in [9], which improved image quality by means of an eigenbeam space division multiplexing (E-SDM) technique and subcarrier allocation based on its signal-to-noise ratio (SNR). A few more approaches are reported in [10, 11]. The methods named above are proved to produce significant gains in image quality, but they cannot support overloaded MIMO scenarios due to rank-deficiency in a channel matrix [12].

The contribution of this paper can be summarized as follows. This paper proposes a novel linear precoding scheme for high-quality video transmission in overloaded MIMO systems, which makes it possible to partially apply the E-SDM transmission to data symbols. Low complexity postcoder is also proposed, which makes use of a linear detector for the E-SDM symbols and the PVC-based non-linear detector for the others. It is demonstrated from simulation results that the proposed precoder surpasses a conventional UPA scheme in terms of peak signal-to-noise ratio (PSNR). In addition, the proposed postcoder reduces the computational complexity by over 61% compared to the conventional PVC-based detector while achieving 40 dB in PSNR and maintaining near-optimal performance when received SNR is higher than 10 dB.

The following notations will be used throughout this paper. The superscripts $(\cdot)^T$ and $(\cdot)^H$ represent transpose and

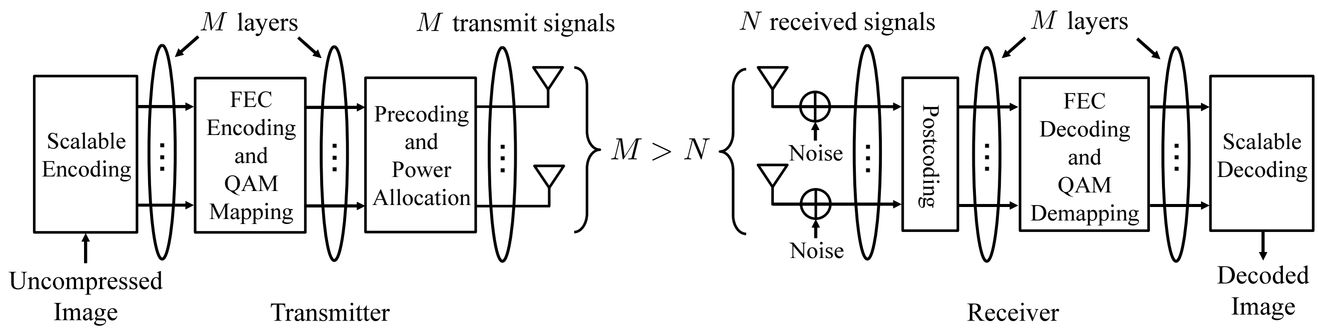

Fig. 1. Overall system for wireless video transmission through overloaded MIMO channels. The number of receive antennas is smaller than that of transmit antennas $(M > N)$.

Hermitian transpose, respectively. $\mathrm{diag}\left(\cdot\right)$ is a diagonal matrix, $\mathbf{O}_{m,n}$ is an $m \times n$ zero matrix, and $\mathbf{I}_m$ is an $m \times m$ identity matrix. $\mathbf{x}_{[a:b]}$ denotes a subvector of $\mathbf{x} = [x_1, \cdots, x_m]$ containing the elements $x_a, \cdots, x_b$. $\mathbf{e}_m$ means a column vector with 1 in the mth position and 0 in every other position.

2. VIDEO TRANSMISSION SYSTEM

Fig. 1 describes a block diagram of the overall system for wireless video transmission through overloaded MIMO channels. The scalable encoding block performs source coding by Motion JPEG 2000, where each video frame is compressed as an independent still image and is transmitted in series. JPEG 2000 encoder produces a scalable code stream which has M quality layers whose contribution to image quality is unequal. Upper layers are more important than lower ones since lower layers are predicted on the foundation of upper ones [13]. The outputs of the scalable encoder are sent to the forward error correction (FEC) encoder, where FEC is separately applied to each layer so as to prevent errors on lower layers from propagating to upper ones. The bit sequences of the FEC encoded layers are mapped to the constellation points of quadrature amplitude modulation (QAM). M QAM symbol sequences are fed to the precoding and power allocation block and finally transmitted through M antennas.

The receiver observes the transmitted signals through the overloaded MIMO channel where the number of receive antennas, denoted by N, is smaller than that of transmit antennas $(M > N)$. Postcoder recovers M transmit symbol sequences from N spatially multiplexed signals.

3. PRECODING AND POSTCODING

3.1. Precoding for Video Transmission

This paper considers the overloaded MIMO system which has M transmit and N receive antennas $(M > N)$. The number of spatial streams and quality layers are also equal to M. Let $\mathbf{H}$ be an $N \times M$ matrix of complex channel coefficients, and the receiver estimates $\mathbf{H}$ and returns it back to the transmitter [14]. Let $\mathbf{s} = [s_1 \cdots s_M]^T$ be the transmit vector made up of M QAM symbols from different layers, and average power per symbol is normalized as 1. The mth element of $\mathbf{s}$, denoted by s_m, corresponds to the symbol on layer m. Hence, s_1 is the most significant information of all M symbols in any transmit vector because the data on layer 1 has the largest contribution to image quality of all. The power allocated to each symbol is controlled by $\mathbf{P} = \mathrm{diag}\left(\sqrt{p_1}, \cdots, \sqrt{p_M}\right)$.

This paper proposes a linear precoder which makes it possible to improve video quality by means of partial E-SDM transmission [15] and decrease the computational complexity required for postcoding at the receiver side. E-SDM, however, is not applicable to rank-deficient channels $(M > N)$. The proposed precoder first applies Householder transformations [16] to reduce $\mathbf{H}$ to the following lower triangular form:

$$\mathbf{H}\mathbf{W}_{\mathrm{H}} = \begin{bmatrix} \multicolumn{3}{c}{\mathbf{L}} & \multicolumn{3}{c}{\mathbf{O}_{R,M-R}} \\ h'_{N,1} & \cdots & h'_{N,R} & h'_{N,N} & \cdots & h'_{N,M} \end{bmatrix}, \quad (1)$$

where $R = N - 1$, $\mathbf{W}_{\mathrm{H}}$ is an $M \times M$ Householder matrix, and $\mathbf{L}$ is an $R \times R$ lower triangular matrix. This triangulation allows the precoder to apply E-SDM to the submatrix $\mathbf{L}$ since $\mathbf{L}$ takes a square form. $\mathbf{L}$ can be factorized by the singular value decomposition as $\mathbf{L} = \mathbf{U}\mathbf{\Sigma}\mathbf{V}^H$, where $\mathbf{U}$ and $\mathbf{V}$ are $R \times R$ unitary matrices, $\mathbf{\Sigma} = \mathrm{diag}\left(\sqrt{\lambda_1}, \cdots, \sqrt{\lambda_R}\right)$, and λ_i denotes the ith largest eigenvalue of $\mathbf{L}^H\mathbf{L}$. The weight matrix for E-SDM transmission can be obtained by $\mathbf{V}$ as

$$\mathbf{W}_{\mathrm{E}} = \begin{bmatrix} \mathbf{V} & \mathbf{O}_{R,M-R} \\ \mathbf{O}_{M-R,R} & \mathbf{I}_{M-R} \end{bmatrix}. \quad (2)$$

Multiplying $\mathbf{H}\mathbf{W}_{\mathrm{H}}$ by $\mathbf{W}_{\mathrm{E}}$ yields

$$\mathbf{H}\mathbf{W}_{\mathrm{H}}\mathbf{W}_{\mathrm{E}} = \begin{bmatrix} \multicolumn{3}{c}{\mathbf{L}\mathbf{V}} & \multicolumn{3}{c}{\mathbf{O}_{R,M-R}} \\ h''_{N,1} & \cdots & h''_{N,R} & h'_{N,N} & \cdots & h'_{N,M} \end{bmatrix}. \quad (3)$$

The columns of $\mathbf{H}\mathbf{W}_{\mathrm{H}}\mathbf{W}_{\mathrm{E}}$ are ordered based on signal-to-interference-plus-noise ratio (SINR) of spatial streams so that the symbols on upper layers would be allocated to high-SINR spatial streams. The SINR of spatial stream m can be calculated as

$$\gamma_m = \begin{cases} \dfrac{\lambda_m p_m}{\sigma_{\mathrm{n}}^2}, & m = 1, \cdots, R \\ \dfrac{\left|h'_{N,m}\right|^2 p_m}{\sum\limits_{j=N, j\neq m}^{M} \left|h'_{N,j}\right|^2 p_j + \sigma_{\mathrm{n}}^2}, & m = N, \cdots, M \end{cases}, \quad (4)$$

where σ_{n}^2 denotes the receiver noise power. Letting $\pi(i)$ return the spatial stream index associated with the ith largest SINR value, SINR-based ordering can be given by the permutation matrix defined as $\mathbf{W}_{\mathrm{P}} = \left[\mathbf{e}_{\pi(1)}, \cdots, \mathbf{e}_{\pi(M)}\right]^T$. The overall precoding matrix including power control can be expressed as $\mathbf{W} = \mathbf{W}_{\mathrm{H}}\mathbf{W}_{\mathrm{E}}\mathbf{W}_{\mathrm{P}}\mathbf{P}$. Keep in mind that the total transmit power depends only on the diagonal matrix $\mathbf{P}$ because $\mathbf{W}_{\mathrm{H}}$ and $\mathbf{W}_{\mathrm{E}}$ are unitary and $\mathbf{W}_{\mathrm{P}}$ is orthogonal.

The received vector $\mathbf{y} = [y_1 \cdots y_N]^T$ can be written as

$$\mathbf{y} = \mathbf{HWs} + \mathbf{z}, \quad (5)$$

in which $\mathbf{z} = [z_1 \cdots z_N]^T$ is a zero-mean circularly symmetric complex Gaussian noise vector with variance of σ_{n}^2. For postcoding, the receiver measures the composite channel matrix $\mathbf{C} = \mathbf{HW}$ that includes the effect of precoding and power control. The proposed precoder only performs the linear operation by $\mathbf{W}$, so the receiver can make use of any postcoder that works for overloaded MIMO channels such as MLD and PVC-based detector [6] in order to acquire $\mathbf{s}$ from Eq. (5).

3.2. Reduced Complexity Postcoding

This paper proposes a reduced complexity postcoder (RCP) which works in cooperation with the proposed precoder. The proposed RCP finds R symbols transmitted by E-SDM with a simple linear approach and the residual $M-R$ symbols with a non-linear approach. Let $\mathbf{C}'$ be the $R\times M$ submatrix obtained by deleting the Nth row from $\mathbf{C}$. $\mathbf{C}'$ is comprised of R non-zero columns and $M-R$ all-zero columns as described in Eq. (3). Here, define the index set of non-zero columns in $\mathbf{C}'$ as $\mathcal{L} = \{l_1, \cdots, l_R\}$, and the index set of all-zero columns in $\mathbf{C}'$ as $\mathcal{N} = \{n_1, \cdots, n_{M-R}\}$. The symbol vectors associated with $\mathcal{L}$ and $\mathcal{N}$ are represented by $\mathbf{s}_{\mathcal{L}} = [s_{l_1} \cdots s_{l_R}]^T$ and $\mathbf{s}_{\mathcal{N}} = \left[s_{n_1} \cdots s_{n_{M-R}}\right]^T$, respectively. First, the proposed RCP estimates $\mathbf{s}_{\mathcal{L}}$ by solving the following linear system:

$$\mathbf{y}_{[1:R]} = \mathbf{C}'_{\mathcal{L}}\mathbf{s}_{\mathcal{L}} + \mathbf{z}_{[1:R]}, \quad (6)$$

where $\mathbf{C}'_{\mathcal{L}} = \left[\mathbf{c}'_{l_1} \cdots \mathbf{c}'_{l_R}\right]$ takes a square form, and $\mathbf{c}'_i$ means the ith column of $\mathbf{C}'$. $\mathbf{y}_{[1:R]}$ does not contain the symbols in $\mathbf{s}_{\mathcal{N}}$ because all the channel coefficients of $\mathbf{C}'$ associated with $\mathbf{s}_{\mathcal{N}}$ are forced to be zero by the precoder. Thus, any conventional linear postcoder such as ZF and MMSE can detect $\mathbf{s}_{\mathcal{L}}$.

The remaining $M-R$ symbols of $\mathbf{s}_{\mathcal{N}}$ can be obtained by solving the following equation:

$$y_N - [c_{l_1} \cdots c_{l_R}]\,\widetilde{\mathbf{s}}_{\mathcal{L}} = \left[c_{n_1} \cdots c_{n_{M-R}}\right]\mathbf{s}_{\mathcal{N}} + z_N, \quad (7)$$

in which c_i means the ith entry in the Nth row of $\mathbf{C}$, and $\widetilde{\mathbf{s}}_{\mathcal{L}}$ is a replica vector created by remapping the symbols of the estimated $\mathbf{s}_{\mathcal{L}}$ to the nearest constellation points. Then, $\widetilde{\mathbf{s}}_{\mathcal{L}}$ is subtracted from y_N to cancel its contribution as interference. Eq. (7) is an underdetermined system because only one equation has $M-R$ unknowns, so it is impossible to solve it by linear approaches. The proposed RCP performs PVC-based MMSE detection to find $\mathbf{s}_{\mathcal{N}}$ from Eq. (7). Details on the PVC approach is given in [6].

4. SIMULATIONS

4.1. Simulations Details

Motion JPEG 2000 is used for encoding and decoding 1920×1080 color images where source coding rate is 1 bpp, and frame rate is 30 fps. A code stream is made up of 4 layers, and each layer has the equivalent length. A total of 100 images [17] are transmitted at every received SNR. Reconstruction quality of the received image is assessed by its PSNR value. This paper defines the perceptually acceptable image quality as the PSNR of over 40 dB. The transmitter sends 4 spatial streams modulated with 4-QAM through 4 antennas and the receiver observes them with 3 antennas. The bandwidth occupied by the system is 80 MHz, and the carrier frequency is 5.2 GHz. Each packet contains the data of all 4 layers, and binary convolutional codes with the coding rate of $3/4$ are used for FEC. Channel model B defined by the task group ac [18] is used for simulations under indoor residential non-line-of-sight scenarios. Other parameters follow the IEEE 802.11ac standard [19]. For comparison, the proposed precoder is used with MLD, PVC-based MMSE detector [6], and the proposed RCP. This paper also presents the results obtained by the conventional simple UPA scheme (Conv. UPA), which supplies a large amount of power to upper layers instead of precoding. In each scheme, power allocation ratio is set to

$$p_1 : p_2 : p_3 : p_4 = \begin{cases} 2^9 : 2^6 : 2^3 : 2^0, & \text{Conv. UPA} \\ 1 : 1 : 1 : 1, & \text{Prop. precoder} \end{cases}. \quad (8)$$

4.2. Results and Discussion

BER on layers versus received SNR curves of the proposed precoder with RCP are plotted in Fig. 2(a). The BER curves on upper layers (important layers) in Fig. 2(a) fall off even more rapidly than those on lower layers due to E-SDM transmission and SINR-based ordering performed by the proposed precoder. BER on layer 1 versus received SNR curves of all the schemes are presented in Fig. 2(b). It is confirmed from Fig. 2(b) that the proposed precoder outperforms Conv. UPA regardless of postcoder choice, and the proposed RCP as well as PVC closely approaches the optimal performance obtained by MLD. Average PSNR versus received SNR curves are depicted in Fig. 3. No large difference can be observed among

Table 1. Computational complexity required for postcoding at the receiver side for the case of 2^B-QAM.

	Number of complex additions	Number of complex multiplications
MLD	$(MN + N - 1)\, 2^{BM}$	$(MN + N)\, 2^{BM}$
PVC	$4N^3 - 2N^2 + N + (2MN - 1)\, 2^{B(M-N)}$	$5N^3 + 5N^2 + 2N + (2MN + N)\, 2^{B(M-N)}$
Prop. RCP	$4N^3 - 13N^2 + (M + 14)\, N - 2M - 4 + (2M - 2N + 1)\, 2^{B(M-N)}$	$5N^3 - 9N^2 + (M + 9)\, N + (2M - 2N + 1)\, 2^{B(M-N)}$

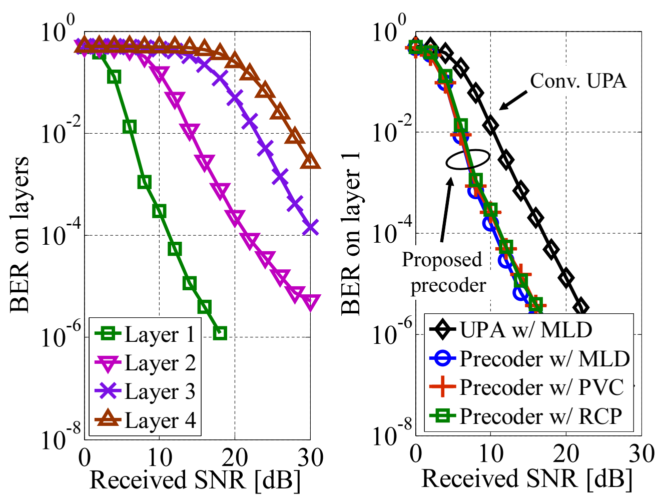

(a) Proposed precoder w/ Prop. RCP (all layers)

(b) All schemes (layer 1)

Fig. 2. BER on layers versus received SNR curves.

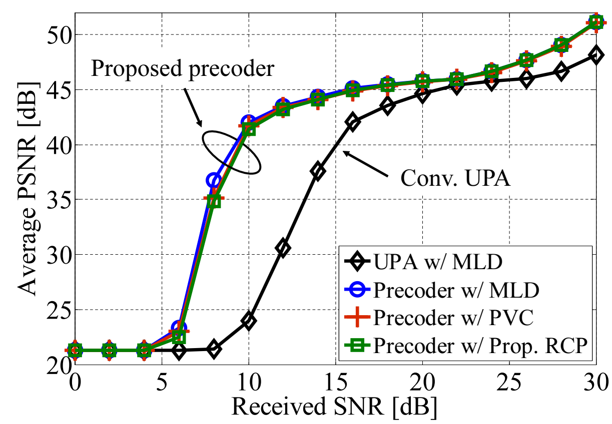

Fig. 3. Average PSNR versus received SNR curves.

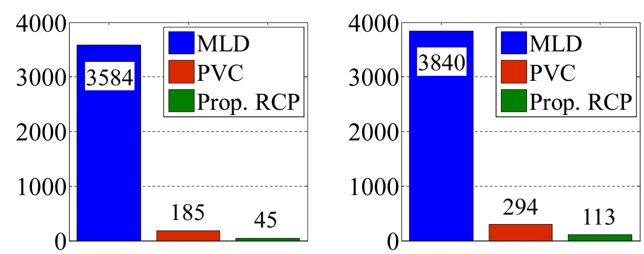

(a) No. of complex additions (b) No. of complex multiplications

Fig. 4. Complexity required for postcoding at the receiver side for the case of $M = 4$, $N = 3$, and $B = 2$ (4-QAM).

PSNR performances of the three postcoders. In particular, the proposed RCP shows almost equivalent performance to MLD when received SNR is higher than 10 dB. It is also shown by Fig. 3 that the proposed precoder surpasses Conv. UPA in PSNR performance at every received SNR value whereas the total transmit power is uniformly distributed among all layers in the proposed precoding scheme. The improvement in PSNR by the proposed precoder compared to Conv. UPA comes up to around 18 dB at SNR of 10 dB. The proposed precoder attains 40 dB in PSNR at SNR values of over 10 dB. Figs. 2(b) and 3 indicate that the lower the BER on layer 1 is, the higher the PSNR performance becomes. In other words, low BER on upper layers directly contributes to the significant PSNR gain produced by the proposed method.

Computational complexity required for postcoding at the receiver side is summarized in Table 1. The computational complexity increases exponentially with M and B for MLD, and with $M - N$ and B for PVC and the proposed RCP. Fig. 4 shows the computational complexity for the case where $M = 4$, $N = 3$, and 4-QAM is used. It is confirmed from Fig. 4 that the proposed RCP requires the least computational complexity of all, and it reduces the number of complex additions by 73% and that of complex multiplications by 61% compared to PVC. This is because the proposed RCP detects $\mathbf{s}_{\mathcal{L}}$ by linear MMSE and $\mathbf{s}_{\mathcal{N}}$ by PVC-based MMSE, which decreases much more complexity than detecting all symbols of $\mathbf{s}$ by PVC-based algorithms.

5. CONCLUSION

This paper has proposed a precoder for video transmission in overloaded MIMO systems, which is predicated on E-SDM and SINR-based ordering. The proposed precoder surpasses Conv. UPA in PSNR at any received SNR. In addition, low complexity postcoder has been proposed, which reduces the number of complex additions and multiplications by 73% and 61% compared to the conventional PVC-based MMSE detector while achieving 40 dB in PSNR and maintaining near-optimal performance when SNR is greater than 10 dB.

6. REFERENCES

[1] A. Goldsmith, S.A. Jafar, N. Jindal, and S. Vishwanath, “Capacity limits of MIMO channels,” *IEEE J. Selected Areas in Commun.*, vol. 21, no. 5, pp. 684–702, June 2003.

[2] K. Sulonen, P. Suvikunnas, L. Vuokko, J. Kivinen, and P. Vainikainen, “Comparison of MIMO antenna conguurations in picocell and microcell environments,” *IEEE J. Selected Areas in Commun.*, vol. 21, no. 5, pp. 703–712, June 2003.

[3] A.A.-H. Azremi, N. Jamaly, K. Haneda, C. Icheln, and V. Viikari, “Design and measurement-based evaluation of multi-antenna mobile terminals for LTE 3500 MHz band,” *Progress In Electromagnetics Research B*, vol. 53, pp. 241–266, 2013.

[4] S.J. Grant and J.K. Cavers, “Performance enhancement through joint detection of cochannel signals using diversity arrays,” *IEEE Trans. Commun.*, vol. 46, no. 8, pp. 1038–1049, August 1998.

[5] L. Bai, C. Chen, and J. Choi, “Lattice reduction aided detection for underdetermined MIMO systems: A prevoting cancellation approach,” in *IEEE Vehicular Technology Conf.*, May 2010.

[6] L. Bai, C. Chen, and J. Choi, “Prevoting cancellation-based detection for underdetermined MIMO systems,” *EURASIP J. Wireless Commun. and Networking*, vol. 2010, September 2010.

[7] X.-W. Chang and X. Yang, “An efficient tree search decoder with column reordering for underdetermined MIMO systems,” in *IEEE Global Telecommun. Conf.*, November 2007.

[8] M.F. Sabir, A.C. Bovik, and R.W. Heath, “Unequal power allocation for JPEG transmission over MIMO systems,” *IEEE Trans. Image Processing*, vol. 19, no. 2, pp. 410–421, February 2010.

[9] K. Tashiro, L. Lanante, M. Kurosaki, and H. Ochi, “High-resolution image transmission over MIMO-OFDM E-SDM system with JSCC,” in *IEEE Int. Conf. on Consumer Electronics-Berlin*, September 2014.

[10] M. Shayegannia, A.H.S. Mohammadi, S. Muhaidat, and M. Torki, “An OFDM based system for transmission of JPEG2000 images using unequal power allocation,” in *IEEE Wireless Commun. and Networking Conf.*, April 2012.

[11] K. Hassan and W. Henkel, “Fast prioritized bit-loading and subcarriers allocation for multicarrier systems,” in *IEEE Vehicular Technology Conf.*, May 2010.

[12] W. Chang, S.-Y. Chung, and Y.H. Lee, “Diversity-multiplexing tradeoff in rank-deficient and spatially correlated MIMO channels,” in *IEEE Int. Symp. on Information Theory*, July 2006.

[13] A. Skodras, C. Christopoulos, and T. Ebrahimi, “The JPEG 2000 still image compression standard,” *IEEE Signal Processing Magazine*, vol. 18, no. 5, pp. 36–58, September 2001.

[14] H. Lou, M. Ghosh, P. Xia, and R. Olesen, “A comparison of implicit and explicit channel feedback methods for MU-MIMO WLAN systems,” in *IEEE Int. Symp. on Personal, Indoor, and Mobile Radio Commun.*, September 2013.

[15] K. Miyashita, T. Nishimura, T. Ohgane, Y. Ogawa, Y. Takatori, and K. Cho, “High data-rate transmission with eigenbeam-space division multiplexing (E-SDM) in a MIMO channel,” in *IEEE Vehicular Technology Conf.*, September 2002.

[16] K.L. Chung and W.M. Yan, “The complex Householder transform,” *IEEE Trans. Signal Processing*, vol. 45, no. 9, pp. 2374–2376, October 1997.

[17] Digital Cinema Initiatives, “StEM access procedures,” *http://www.dcimovies.com/StEM/*, May 2017.

[18] G. Breit, H. Sampath, S. Vermani, R.V. Nee, and M. Cheong et al., “TGac channel model addendum,” *IEEE 802.11-09/0308r12*, March 2010.

[19] IEEE Std 802.11ac$^{\text{TM}}$ 2013, “Part 11: Wireless LAN medium access control (MAC) and physical layer (PHY) specifications, amendment 4: enhancements for very high throughput for operation in bands below 6 GHz,” December 2013.